Causes of and Solutions to Wind Speed Bias in NREL's 2020 Offshore Wind Resource Assessment for the California Pacific Outer Continental Shelf

Nicola Bodini,[1] Mike Optis,[2] Ye Liu,[3] Brian Gaudet,[3] Raghavendra Krishnamurthy,[3] Andrew Kumler,[1] David Rosencrans,[4] Alex Rybchuk,[1] Sheng-Lun Tai,[3] Larry Berg,[3] Walter Musial,[1] Julie K. Lundquist,[1,4,5] Avi Purkayastha,[1] Ethan Young,[1] and Caroline Draxl[1,5]

1 National Renewable Energy Laboratory
2 Veer Renewables Inc.
3 Pacific Northwest National Laboratory
4 Department of Atmospheric and Oceanic Sciences, University of Colorado Boulder
5 Renewable and Sustainable Energy Institute

NREL is a national laboratory of the U.S. Department of Energy
Office of Energy Efficiency & Renewable Energy
Operated by the Alliance for Sustainable Energy, LLC

This report is available at no cost from the National Renewable Energy Laboratory (NREL) at www.nrel.gov/publications.

Contract No. DE-AC36-08GO28308

Technical Report
NREL/TP-5000-88215
PNNL-35708
February 2024

Causes of and Solutions to Wind Speed Bias in NREL's 2020 Offshore Wind Resource Assessment for the California Pacific Outer Continental Shelf

Nicola Bodini,[1] Mike Optis,[2] Ye Liu,[3] Brian Gaudet,[3] Raghavendra Krishnamurthy,[3] Andrew Kumler,[1] David Rosencrans,[4] Alex Rybchuk,[1] Sheng-Lun Tai,[3] Larry Berg,[3] Walter Musial,[1] Julie K. Lundquist,[1,4,5] Avi Purkayastha,[1] Ethan Young,[1] and Caroline Draxl[1,5]

1 National Renewable Energy Laboratory
2 Veer Renewables Inc.
3 Pacific Northwest National Laboratory
4 Department of Atmospheric and Oceanic Sciences, University of Colorado Boulder
5 Renewable and Sustainable Energy Institute

Suggested Citation
Bodini, Nicola, Mike Optis, Ye Liu, Brian Gaudet, Raghavendra Krishnamurthy, Andrew Kumler, David Rosencrans, Alex Rybchuk, Sheng-Lun Tai, Larry Berg, Walter Musial, Julie K. Lundquist, Avi Purkayastha, Ethan Young, and Caroline Draxl. 2024. *Causes of and Solutions to Wind Speed Bias in NREL's 2020 Offshore Wind Resource Assessment for the California Pacific Outer Continental Shelf*. Golden, CO: National Renewable Energy Laboratory. NREL/TP-5000-88215. https://www.nrel.gov/docs/fy24osti/88215.pdf.

NREL is a national laboratory of the U.S. Department of Energy
Office of Energy Efficiency & Renewable Energy
Operated by the Alliance for Sustainable Energy, LLC

This report is available at no cost from the National Renewable Energy Laboratory (NREL) at www.nrel.gov/publications.

Contract No. DE-AC36-08GO28308

Technical Report
NREL/TP-5000-88215
PNNL-35708
February 2024

National Renewable Energy Laboratory 15013 Denver West Parkway Golden, CO 80401
303-275-3000 • www.nrel.gov

NOTICE

This work was authored in part by the National Renewable Energy Laboratory, operated by Alliance for Sustainable Energy, LLC, for the U.S. Department of Energy (DOE) under Contract No. DE-AC36-08GO28308. Funding provided by the U.S. Department of Energy Office of Energy Efficiency and Renewable Energy Wind Energy Technologies Office. The views expressed herein do not necessarily represent the views of the DOE or the U.S. Government.

Cover Photos by Dennis Schroeder: (clockwise, left to right) NREL 51934, NREL 45897, NREL 42160, NREL 45891, NREL 48097, NREL 46526.

List of Acronyms

a.s.l.	above sea level
BOEM	Bureau of Ocean Energy Management
cRMSE	centered (unbiased) root-mean-square error
CA20	20-year wind resource data set produced in 2020 by NREL for the California OCS
CFSv2	Coupled Forecast System model version 2
COAMPS	Coupled Ocean Atmosphere Mesoscale Predictive System
GHI	global horizontal irradiance
HYCOM	HYbrid Coordinate Ocean Model
km	kilometer
m/s	meter per second
MERRA-2	Modern-Era Retrospective analysis for Research and Applications, Version 2
MUR	MUlti-sensor high-Resolution
MYNN	Mellor-Yamada-Nakanishi-Niino
NARR	North American Regional Reanalysis
NOAA	National Oceanic and Atmospheric Administration
NOW-23	2023 National Offshore Wind (data set)
NREL	National Renewable Energy Laboratory
OCS	outer continental shelf
OSTIA	Operational Sea Surface Temperature and Ice Analysis
PBL	planetary boundary layer
PNNL	Pacific Northwest National Laboratory
RAP	Rapid Refresh
ROMS	Regional Ocean Modeling System
SST	sea surface temperature
W/m^2	watt per square meter
WRF	Weather Research and Forecasting (model)
YSU	Yonsei University

Executive Summary

This report provides the results of a detailed analysis of the causes of high wind speed bias in the 20-year wind resource data set for offshore California that the National Renewable Energy Laboratory (NREL) released in 2020, herein called CA20. The data set was developed using the state-of-the-art Weather Research and Forecasting model. Notably, no floating lidars were available at the time in offshore California to validate offshore hub-height wind speeds.

In late 2020, the Pacific Northwest National Laboratory (PNNL) deployed two floating lidars in the California Outer Continental Shelf, near the Bureau of Ocean Energy Management (BOEM) call areas of Humboldt and Morro Bay. Using these observations through 2021, NREL found considerable bias in modeled hub-height winds at both locations: up to +2 m/s at Humboldt over a 6-month period, and up to +1 m/s at Morro Bay over a 1-year period. Upon the discovery of this bias, the U.S. Department of Energy and BOEM funded NREL and PNNL to investigate the causes of, impacts of, and solutions to the bias in the CA20 data set. This report summarizes the findings of this research.

We first investigated whether different Weather Research and Forecasting model setups could lead to reduced bias. We found that the choice of planetary boundary layer (PBL) scheme—which controls the vertical turbulent mixing of momentum, heat, and moisture in the lowermost part of the atmosphere—greatly affected hub-height wind speeds in the region. Specifically, switching from the Mellor-Yamada-Nakanishi-Niino (MYNN) scheme used in CA20 (and widely used across a range of operational and research weather models) to the less common Yonsei University (YSU) scheme nearly eliminated the bias at both the Humboldt and Morro Bay lidar locations.

The large discrepancy between the MYNN- and YSU-modeled hub-height winds highlighted the role of atmospheric stability. In general, PBL schemes agree well in conditions of high turbulence and mixing, normally referred to as “unstable” conditions. By contrast, PBL schemes start to diverge in “stable” conditions, where turbulence is low and thermal stratification (i.e., higher-temperature air sitting on top of colder air) greatly suppresses vertical mixing. Under such conditions, winds aloft can decouple from surface effects and greatly accelerate, causing high wind speeds at hub height and frequent low-level jets. We determined that these stable conditions are in fact dominant in offshore California. The region is characterized by moderate-to-extreme stable stratification with a low-level jet *on average* around 200 meters above sea level. To our knowledge, no wind energy area globally has as strongly stable stratification as offshore California. Under these extreme conditions, we determined that the MYNN scheme models higher stability than YSU, resulting in less vertical turbulent mixing than YSU and allowing for the acceleration of hub-height winds, more intense low-level jets, and higher-amplitude inertial oscillations. Using surface observations, we found that MYNN overestimates near-surface stability, whereas YSU tends to model stability better.

We then considered several short-term case studies to assess additional meteorological drivers of the bias at Humboldt. We found that during synoptic-scale northerly flows driven by the North Pacific High and inland thermal low, a coastal warm bias in the MYNN case studies contributes to the modeled wind speed bias by altering the boundary layer thermodynamics via a thermal wind mechanism.

Given the strong performance of the YSU-based runs in offshore California, NREL has produced and published an updated version of the CA20 data set with YSU as the PBL scheme. This updated data set is now part of NREL's 2023 National Offshore Wind (NOW-23) data set, which covers all U.S. offshore waters. The development and final validation of the NOW-23 data set in offshore California is documented in this report.

More broadly, the performance of MYNN in extremely stable conditions is concerning. Given that the atmospheric science community has largely embraced MYNN as the go-to PBL scheme (e.g., it is the scheme used in the National Oceanic and Atmospheric Administration's High-Resolution Rapid Refresh model and the New European Wind Atlas), additional research is needed to understand how and why such large biases occur and whether they occur in other locations around the world.

Table of Contents

List of Figures

List of Tables

1 Introduction

In 2020, the National Renewable Energy Laboratory (NREL) produced and published a 20-year offshore wind resource assessment for the California Pacific Outer Continental Shelf (OCS) (Optis et al. 2020), named "CA20." CA20 was produced using the Weather Research and Forecasting (WRF) model. As for all numerical weather prediction models, different choices exist when it comes to the determination of the specific model setup to use in a given region. For the CA20 data set, the WRF setup was chosen after a validation against observations from an array of near-surface buoys and coastal radars and based on results for a sister data set for the mid-Atlantic region, which was validated against observations from two floating lidars. Optis et al. (2020) describe the validation performed and the resulting final model setup. Notably, floating lidars, which offer optimal observations (i.e., those collected at heights of interest for wind energy and far enough from the coast), were not available in the region when this validation was performed and the model setup was chosen. In 2020, the Pacific Northwest National Laboratory (PNNL) deployed two floating lidars (Krishnamurthy et al. 2023) in the California OCS, near the Bureau of Ocean Energy Management (BOEM) call areas of Humboldt and Morro Bay (Figure 1).

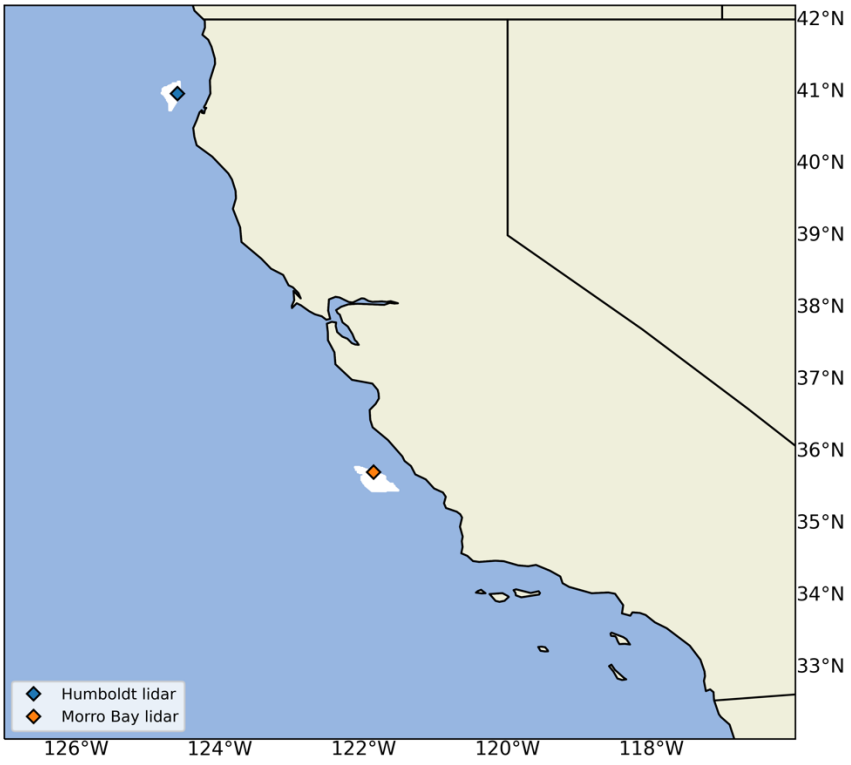

Figure 1. Locations of the two floating lidars in the California OCS. The white areas show the current BOEM wind energy areas in the region.

Given the deployment of the lidars in the region, BOEM funded NREL to validate the CA20 model setup against the lidar measurements. The results of this comparison are summarized in Bodini et al. (2022), and reveal a significant bias between modeled and observed data, especially

over the 6 months of available observations at Humboldt (Figure 2, taken from Bodini et al. [2022]).

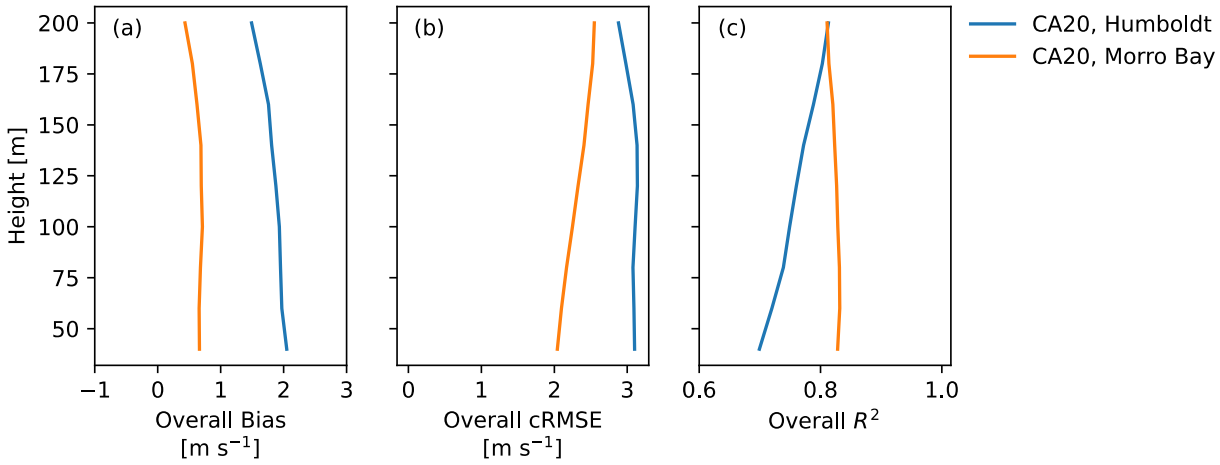

Figure 2. (a) Bias, (b) centered root-mean-square error (cRMSE), and (c) correlation coefficient R^2 calculated at Humboldt and Morro Bay for the CA20 validation run compared to the floating lidar observations. (Figure taken from Bodini et al. [2022])

Research performed in late 2022—the results of which are included in Bodini et al. (2022)—revealed that the long-term bias at Humboldt will not be as high as that observed during this validation period of record. In that report, we showed that the validation period was highly anomalous, resulting in very high wind speeds in the 1-year WRF simulation used for the lidar validation. When the simulated data are long-term corrected using reanalysis data and the measure-correlate-predict method, we found that the CA20 data set will have a long-term wind speed bias of roughly 1 meter per second (m/s) on average at both Humboldt and Morro Bay. Further, we found that most of this bias occurs at high wind speed regimes, and in the wind speed regimes that matter most to wind energy (i.e., 5–10 m/s), the bias is more moderate.

Still, given the significant discrepancy between the CA20 model and the lidar observations in the region, BOEM and the U.S. Department of Energy funded NREL and PNNL to investigate the causes of this bias. In this report, we summarize the results of this physical investigation as well as the development and production of an updated wind resource assessment product for the California OCS.

2 Investigating the Causes of Bias

To identify and understand the causes of the wind speed bias found in CA20, we investigated several aspects that can have an impact on the reported modeled wind speed. In the next several sections, we summarize our analysis for each of the considered factors.

2.1 Validation of Sea Surface Temperature

Biases in modeled sea surface temperature (SST) can lead to mischaracterizations of atmospheric stability aloft and influence the wind profile, and several satellite-based SST products are available to use as bottom boundary conditions in numerical weather prediction models. Therefore, we validated the modeled SST product used in CA20 (Operational Sea Surface Temperature and Ice Analysis [OSTIA]) against available observations and compared its accuracy to other SST products at the location of the two floating lidars in the region. We considered the following list of commonly used SST data sets:

- The HYbrid Coordinate Ocean Model (HYCOM) SST product
- The Coupled Ocean Atmosphere Mesoscale Predictive System (COAMPS) Regional Ocean Modeling System (ROMS) SST product
- The University of California Los Angeles CA-ROMS SST product
- The MUlti-sensor high-Resolution (MUR) SST product
- The OSTIA SST product, which was originally adopted as the bottom boundary condition in CA20.

The two SST data products that showed the highest correlations with SST observations at the Humboldt and Morro Bay buoys were the COAMPS ROMS and OSTIA products. Figure 3 shows the correlation statistics between the OSTIA SST and concurrent buoy observations at both the Humboldt and Morro Bay locations for the duration of the lidar deployments. Given the OSTIA product's strong performance, and considering that the COAMPS ROMS product is not available over the full temporal extent of the 20-year CA20 simulations, it was confirmed that the OSTIA SST product is the most appropriate choice for the CA20 simulations.

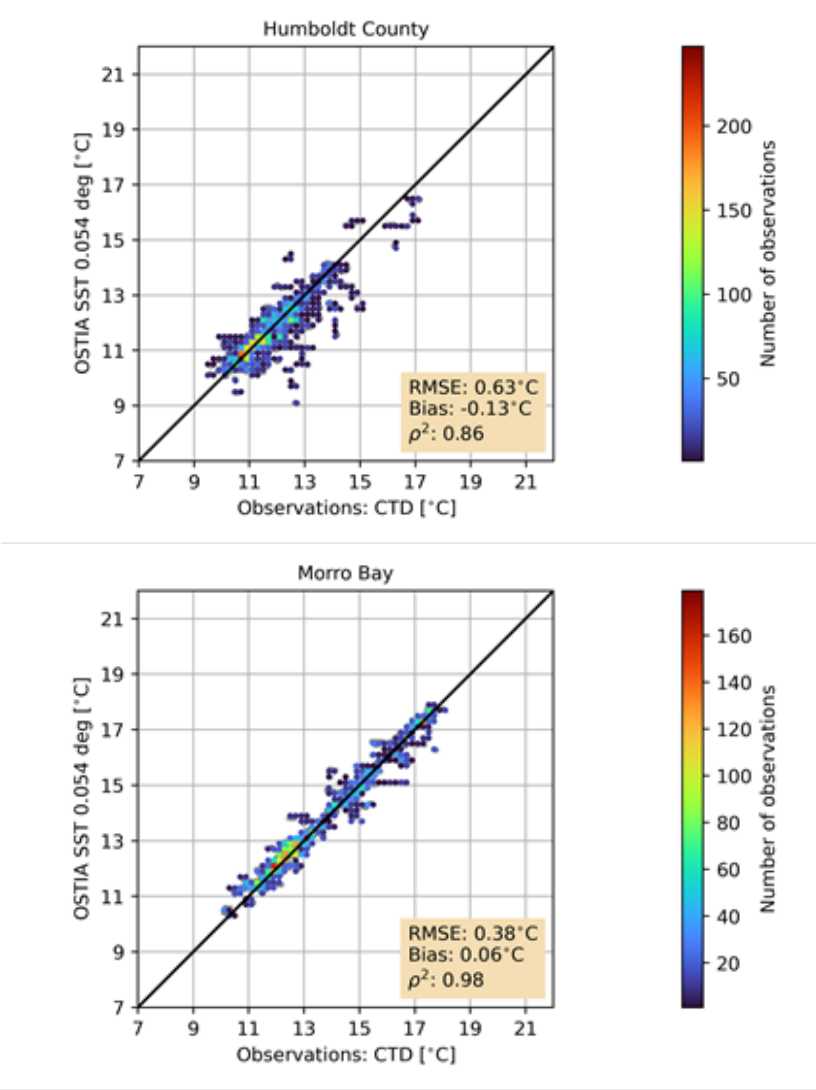

Figure 3. Scatterplot of OSTIA SST compared to observations derived from the buoy conductivity, temperature, and depth (CTD) measurements at Humboldt (top) and Morro Bay (bottom).

2.2 Impact of Reanalysis Product

Reanalysis products provide the boundary forcings to WRF simulations and are key drivers of wind speed. CA20 used the state-of-the-art ERA5 reanalysis product. However, it is possible that this product does not perform well in offshore California, and that such underperformance could be a contributing factor to the CA20 wind speed bias. Therefore, we assessed the accuracy of ERA5 against other products.

Sheridan et al. (2022) used data from the Humboldt and Morro Bay lidar buoy deployments to evaluate the skill of different analysis and reanalysis products in predicting offshore hub-height wind speeds in a manner similar to the East Coast evaluation of Sheridan et al. (2020). The products considered in the analysis are:

- ERA5

- The Coupled Forecast System model version 2 (CFSv2)
- The Modern-Era Retrospective analysis for Research and Applications, Version 2 (MERRA-2) reanalysis product
- The North American Regional Reanalysis (NARR)
- The Rapid Refresh (RAP) analysis product.

As found in that study, for nearly every model and evaluation method, there were negative biases for hub-height wind speed, though the exact bias varied considerably based on model and buoy location. For Humboldt, CFSv2 and MERRA-2 had the lowest-magnitude biases while NARR had the highest magnitude, which might be related to how each analysis represents the modulation of the wind field by the configuration of the local coastline. For Morro Bay, NARR and ERA5 had the lowest-magnitude biases while MERRA-2 had the greatest. Meanwhile, while not superior in terms of overall model bias, RAP tended to have the best centered root-mean-square error (cRMSE) scores and correlation coefficients, consistent with findings from the East Coast study, suggesting that these scores respond favorably to the greater horizontal resolution in RAP than in the other products.

While these results suggest some potential benefit of using RAP as the meteorological driver for these simulations, a disadvantage of RAP is that it is an analysis rather than a reanalysis product, and its internal physics has been continually updated with time, leading to complications for interpreting multiyear simulations using it as a driver.

In addition to the considerations already mentioned, we performed a 4-month comparison of wave spectra predicted by a stand-alone WaveWatch3 simulation as driven by different meteorological analysis and reanalysis products, including the RAP analysis. The simulations were validated with observations from the Morro Bay lidar buoy deployment, along with a nearby National Buoy Data Center buoy. Overall, little difference in modeling skill for wave height and period could be attributed to the use of different analysis meteorological drivers (e.g., the cRMSE for significant wave height at Morro Bay was 0.42 m for both the RAP and the CFS analysis, and 0.43 m for ERA5).

We also directly compared hub-height wind speeds between WRF model simulations of selected cases from the lidar buoy deployments using both RAP and CFS as meteorological drivers (providing the initial conditions for a two-domain configuration, along with the lateral boundary conditions and the analysis nudging target for the coarse domain). Again, little systematic improvement, if any, was found using the RAP product. In Figure 4, we see that for the atmospheric river case of January 27, 2021, the CFS-nudged d01 better matches the lidar buoy observations than the RAP-nudged d01 during the wind ramp associated with the frontal passage, and both domains from the CFS-based simulation appear to match the observations better than the RAP-based simulation in the post-frontal period. It was thus concluded that the long-term model biases were likely not sensitive to the choice of meteorological driver.

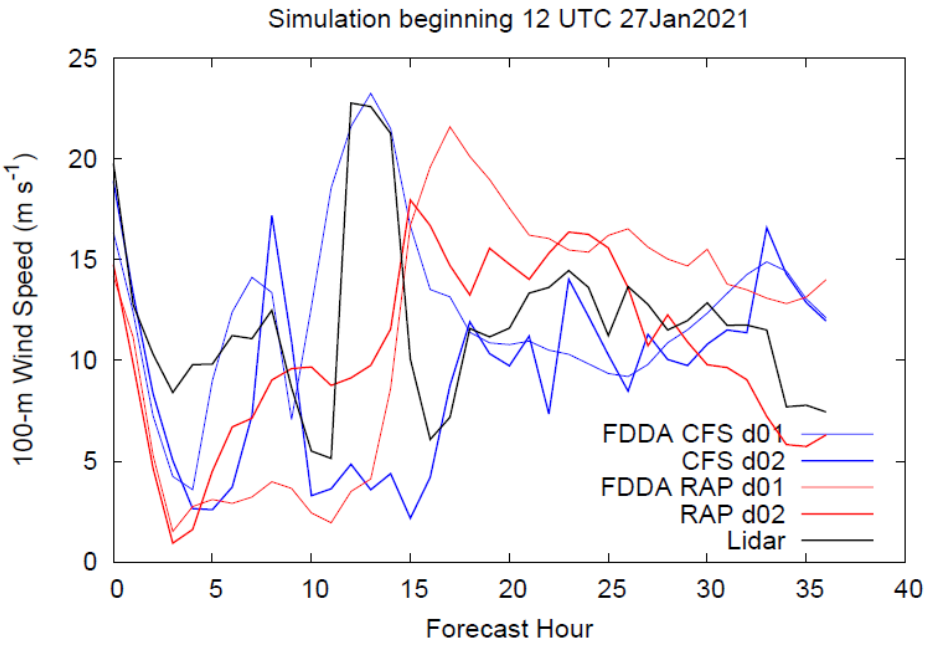

Figure 4. Comparison of 100-m wind speeds observed between 12 UTC on January 27, 2021, and 00 UTC on January 29, 2021, at the Morro Bay lidar buoy (black), and those in the CFS-driven (blue) and RAP-driven (red) WRF simulations for the same period. In the WRF simulations, d01 has 9-kilometer (km) grid spacing and is analysis-nudged to the meteorological driver analysis; d02 is a 3-km nest that is not nudged.

It was thus concluded that the model biases were likely not sensitive to the choice of meteorological driver, and the sensitivity would be expected to decrease with increasing forecast time away from the initial condition. Nevertheless, it should be acknowledged that a more definitive statement on the sensitivity of the simulations to meteorological driver would require more analysis over a substantially greater number of case days.

2.3 Impact of the Choice of the Planetary Boundary Layer Scheme and Atmospheric Stability

Next, we explored the impact that the planetary boundary layer (PBL) scheme in WRF could have on the wind speed bias. Generally speaking, PBL schemes control how momentum, temperature, and moisture are vertically mixed in the lower portion of the atmosphere. Extensive research has shown that the choice of PBL scheme can have significant impact on modeled wind speeds at typical wind turbine hub heights.

Preliminary results already presented in Bodini et al. (2022) revealed how the choice of the PBL scheme has a significant impact on the modeled hub-height winds in offshore California. To investigate this, we ran a 1-year (October 2020–September 2021) WRF simulation using the same WRF setup selected for CA20, but with a different PBL scheme—the Yonsei University (YSU) scheme instead of the Mellor-Yamada-Nakanishi-Niino (MYNN) scheme. We then compared the WRF-simulated wind speed with the lidar observations, using the same process described for the main validation analysis in Bodini et al. (2022). We found that the WRF simulation that adopts the YSU PBL scheme has a significantly reduced bias, both at Humboldt and Morro Bay.

To understand why YSU performs significantly better than MYNN, we began by looking at mean wind profiles over the full year of simulations at both Humboldt and Morro Bay, shown in Figure 5. Here we see low-level jets on average at both locations and for both PBL schemes. We noticed that the MYNN-based simulations have higher wind speeds below 400 m compared to YSU, as well as a stronger jet and lower jet height.

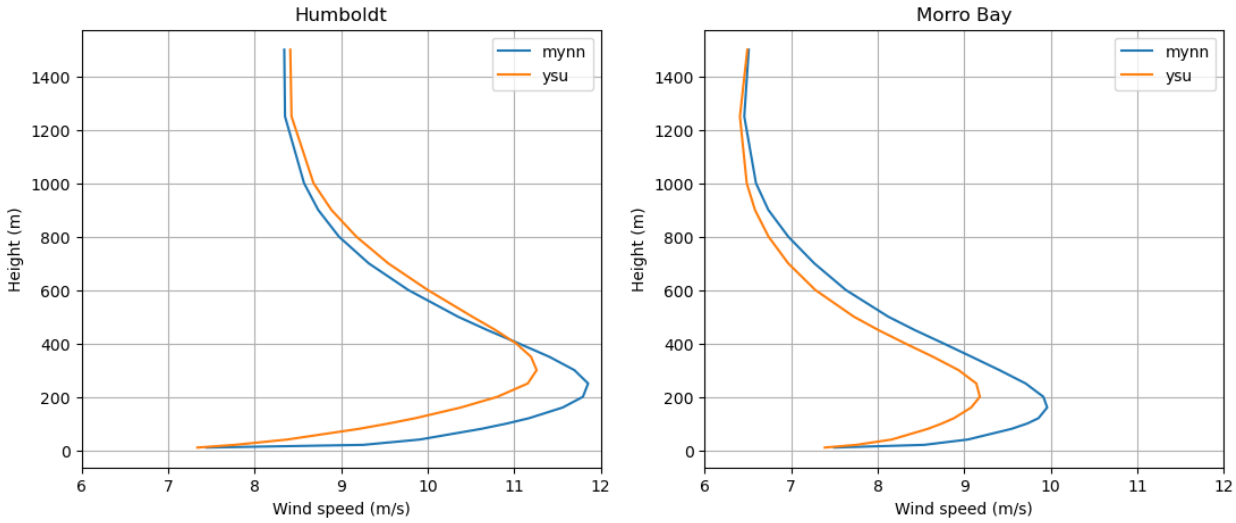

Figure 5. Mean modeled wind profiles for October 2020–September 2021 at Humboldt and Morro Bay using both the MYNN and YSU PBL schemes.

These mean low-level jets, combined with the deviations between MYNN and YSU, both point toward the role of atmospheric stability in explaining the MYNN-based bias. Generally, atmospheric stability describes the degree to which air can move vertically, which is controlled through turbulence. A schematic is shown in Figure 6. During a hot summer day, strong surface heating heats the air immediately above the surface, causing it to become less dense and rise. Cold air aloft comes down to replace the rising hot air and, as this cycle repeats, intense vertical turbulent mixing occurs throughout the lower PBL. Later at night, as the surface cools, the opposite happens: the near-surface air cools first, becomes denser, and becomes trapped below the warmer air aloft, so that vertical turbulent mixing is suppressed.

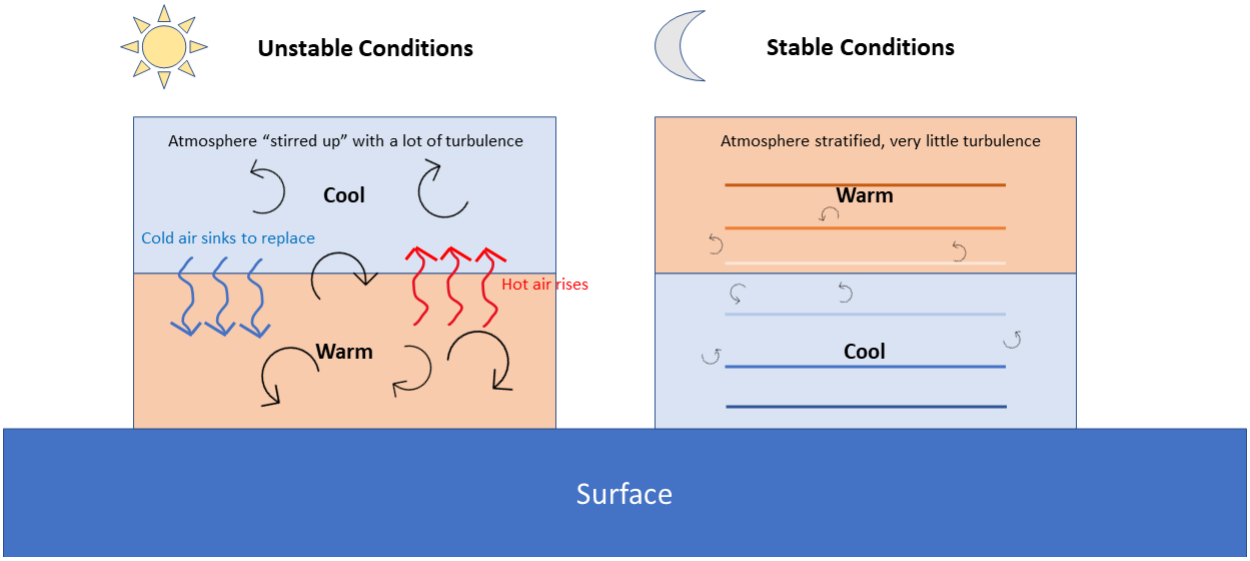

Figure 6. Schematic of unstable and stable conditions and the impact on turbulence and temperature stratification in the PBL

The impact of strong vertical mixing (or lack thereof) on wind profiles is illustrated in Figure 7. In unstable conditions, strong vertical mixing brings momentum from the stronger winds aloft down near the surface, resulting in low wind shear. In stable conditions, the suppression of vertical mixing results in high momentum staying aloft and little getting to the surface, and therefore strong wind shear. Under extremely stable conditions, a low-level jet can form at around 100–300 m above ground.

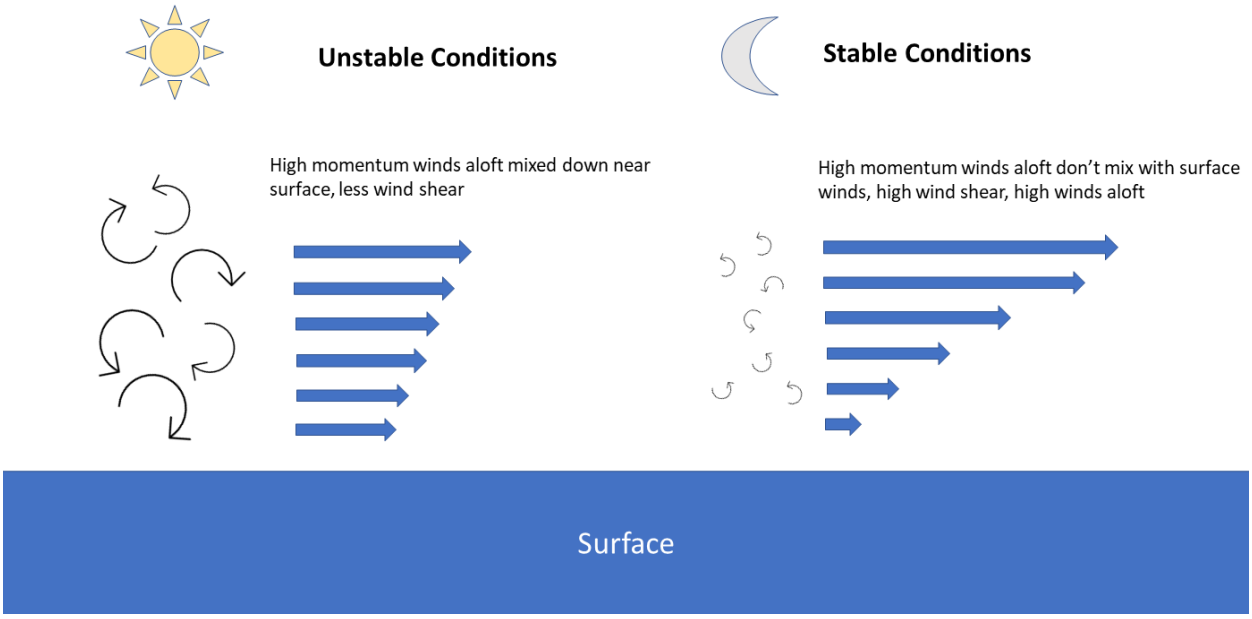

Figure 7. Schematic showing the impact of atmospheric stability on wind profiles

Given the divergence of YSU and MYNN and the mean low-level jets, we posit that conditions at both Humboldt and Morro Bay must be strongly stable on average. This is confirmed in Figure 8, where we plot mean vertical profiles of the potential temperature vertical gradient. We see that the mean gradient is always above zero (i.e., stable conditions), apart from the YSU scheme below 50 m at Morro Bay. We also see that MYNN consistently models higher stability conditions (i.e., larger, positive values of the gradient) below 250 m, especially at Humboldt.

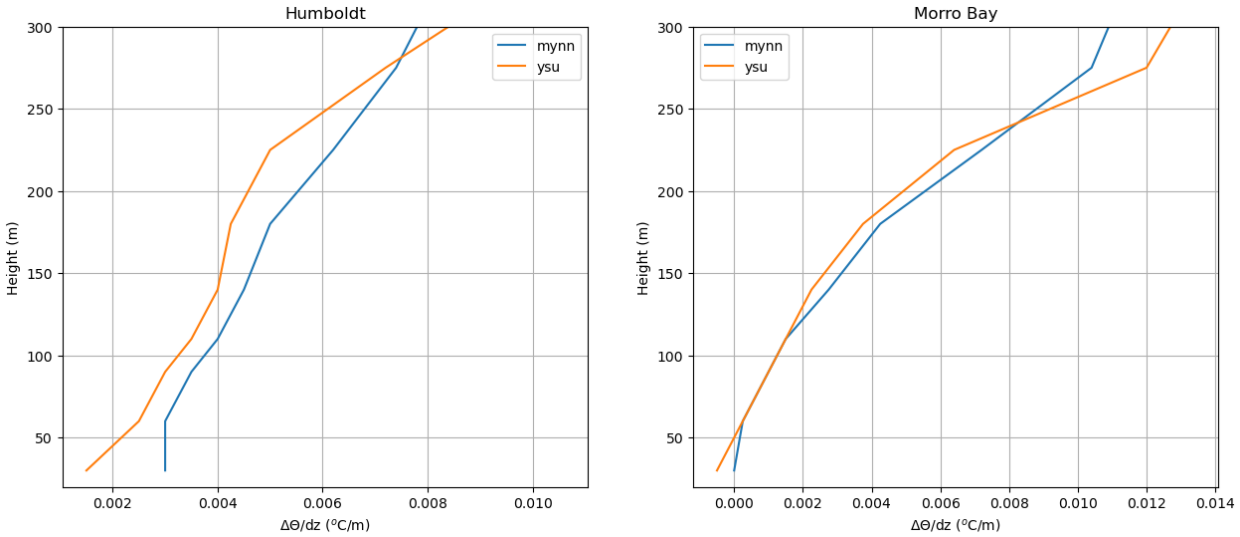

Figure 8. Mean profiles of the modeled potential temperature vertical gradient at both locations and for both PBL schemes

In summary, we find that the PBL scheme has a dramatic impact on the wind speed bias at both Humboldt and Morro Bay. At Humboldt, which is subject to strongly stable conditions on average, the MYNN scheme models stronger stable stratification, resulting in higher wind shear and a stronger and lower low-level jet compared to YSU. The result is a strong positive bias in the MYNN-modeled wind speeds at hub height. At Morro Bay, conditions appear less stable than Humboldt, and MYNN only moderately overestimates stability relative to YSU. Here, the bias in MYNN-modeled wind speeds is lower.

2.4 Validation of Near-Surface Atmospheric Stability

The previous section showed how a key driver of wind profiles is atmospheric stability: in very stable conditions in particular, high wind shear and LLJs are commonly observed. Therefore, validating the modeled atmospheric stability against observations is the natural next step to confirm the main cause for the modeled bias. Ideally, one would want to validate atmospheric stability at the height of interest for wind energy purposes. However, that would require observations of the vertical profile of thermodynamic properties, which are not available in the region. On the other hand, such a comparison can be carried out near the sea surface. Comparing modeled and observed near-surface atmospheric stability can still provide important insights into which of our model simulations is capturing surface conditions more accurately. In fact, surface conditions can play an important role in the formation and shape of the vertical wind profile: If a model simulation cannot correctly re-create the physics near the surface, other phenomena in the lower boundary layer are less likely to be re-created as well.

Multiple approaches exist to estimate atmospheric stability, each with its own strengths and weaknesses. The air-sea temperature difference is the easiest proxy to calculate stability near the surface, where an air-sea temperature difference > 0 suggests stable conditions and an air-sea temperature difference < 0 points toward unstable conditions. The weakness with this method is that wind is not considered in the calculation. Winds help drive stability in the boundary layer, where strong winds increasing with height are often indicative of stable conditions and weaker winds of unstable conditions (where buoyancy can dominate).

A more encompassing method for assessing atmospheric stability is by calculating the Obukhov length (L). The Obukhov length incorporates the surface roughness together with the surface heat flux, where generally positive values represent stable conditions and negative values represent unstable conditions. While more specific stability bins can be used with the Obukhov length (Muñoz-Esparza et al. 2012), for this study we only consider the general stability bins of stable, unstable, and near-neutral conditions. We consider stable conditions when $0 \text{ m} < L < 100 \text{ m}$, unstable conditions when $-100 \text{ m} < L < 0 \text{ m}$, and near-neutral conditions otherwise.

One of the more comprehensive methods to assess stability is by calculating the bulk Richardson number. The bulk Richardson number captures both the wind shear and buoyancy component of stability, all while considering the moisture content of the layer in question. Bulk Richardson numbers were calculated for both Humboldt and Morro Bay, with values generally agreeing with the Obukhov length measure of stability (not shown). However, the humidity sensor on the Morro Bay buoy often malfunctioned during the measurement campaign and thus limited the temporal coverage of the bulk Richardson number at the site. We therefore use the Obukhov length as the main stability metric for this portion of the analysis.

2.4.1 Near-Surface Stability at Humboldt

The top panel in Figure 9 shows the Obukhov length stability class results for the buoy observations and the two WRF model simulations at Humboldt. Observations show stable conditions occurring 51.1% of the time and unstable conditions occurring for 36.8% of the time. The MYNN simulation overestimates stability at the buoy by roughly 6.5%, whereas the YSU simulation falls more in line with the observations, underestimating stability by less than 1%. This validation confirms the overestimation of stability by the MYNN simulation, which leads to more frequent increased wind speeds at heights relevant for wind energy, as any form of buoyancy is overpowered by wind shear near the surface.

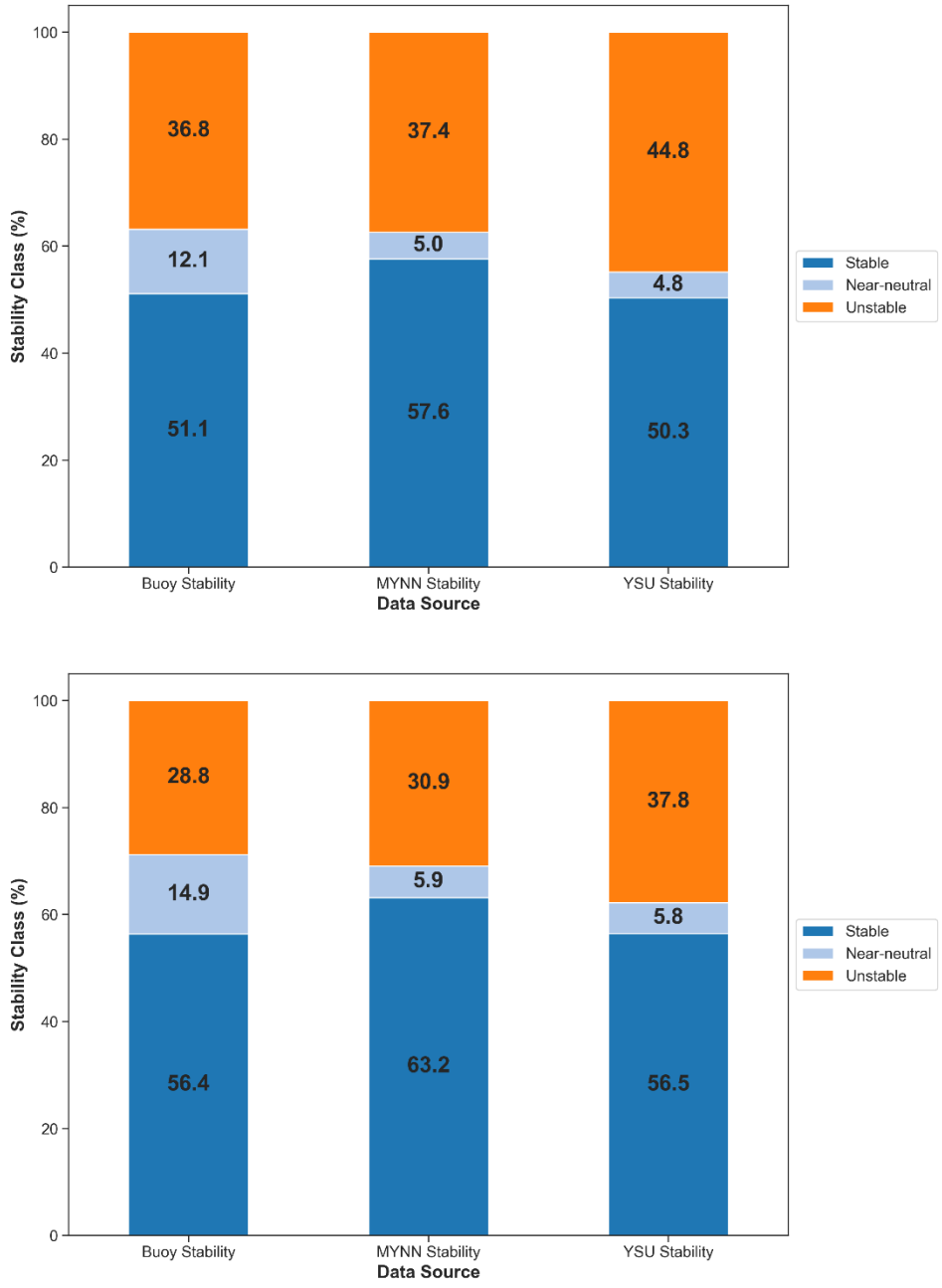

Figure 9. Stability bins for Humboldt during all wind conditions (top) and the dominant wind direction (northerly, bottom)

To further explore the interaction of winds and near-surface stability, the bottom panel in Figure 9 shows the stability bins during times of northerly winds, which are the dominant condition at the site and often coincide with low-level jet formation at Humboldt and are therefore even more stable. Once again, we see that MYNN overestimates the frequency of stable conditions, whereas YSU closely matches the observed distribution.

2.4.2 Near-Surface Stability at Morro Bay

The wind climatology at Morro Bay is similar to that recorded at Humboldt but with a slightly larger component of westerly winds. Northerly winds still dominate, roughly 61% of the time according to the lidar buoy, with westerly winds occurring 26% of the time. Despite the similar wind direction regimes to Humboldt, near-surface stability is rather different. Figure 10 (top) shows near-surface stability bins for all wind directions, and the bottom panel reports near-surface stability during the dominant northerly wind conditions. Unstable conditions dominate at Morro Bay, accounting for nearly 60% of instances in both all and northerly wind directions. MYNN does a reasonable job capturing unstable conditions but still struggles to correctly model stable conditions. On the other hand, YSU is capable of capturing stable conditions well. The reduced frequency of stable conditions at this site can explain why the overall CA20 bias at Morro Bay is lower than that found at Humboldt, where stable conditions are dominant.

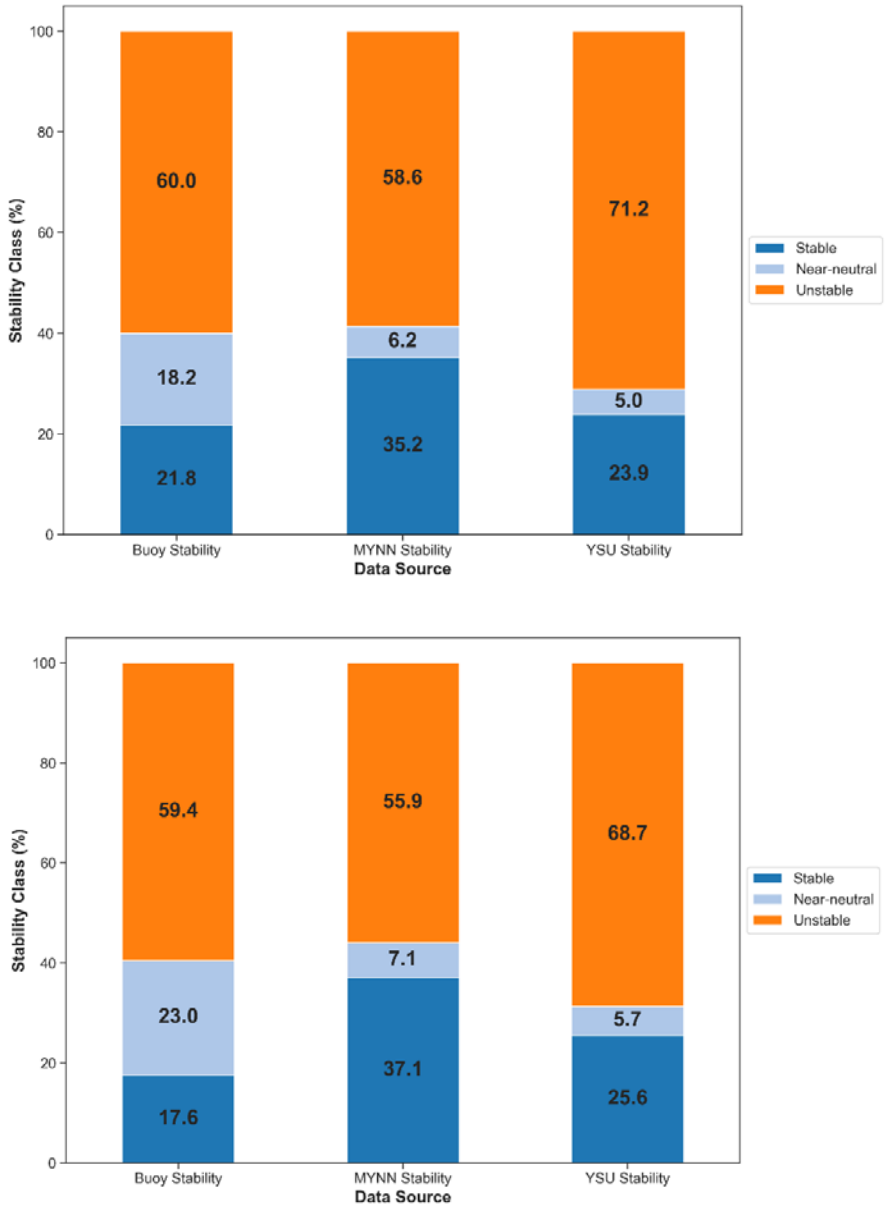

Figure 10. Stability bins for Morro Bay during (top) all wind conditions and (bottom) the dominant wind direction (northerly)

2.5 Impact of Lidar Data Availability

No meteorological instrument can provide a perfect data set—in the real world, data availability will always be less than 100%. Therefore, we characterized in detail the data availability of the two floating lidars used for model validation to provide a broader perspective on the results of such validation. The observations from both lidars come with a metric showing the data availability at each time stamp. We find that both lidars had data availability greater than 80% (i.e., the data quality threshold used in the CA20 validation analysis in Bodini et al. [2022]) for the vast majority of their periods of record. Figure 11 illustrates the frequency of occurrence of several lidar data availability bins at each height. We find that at least 90% of the lidar data at

each height had data availability greater than 80%. This result helps ensure that the lidar data were robust (and therefore used in the validation analysis) the vast majority of the time, so it is highly unlikely that the overall CA20 bias would be much different if the lidars had great data availability all the time.

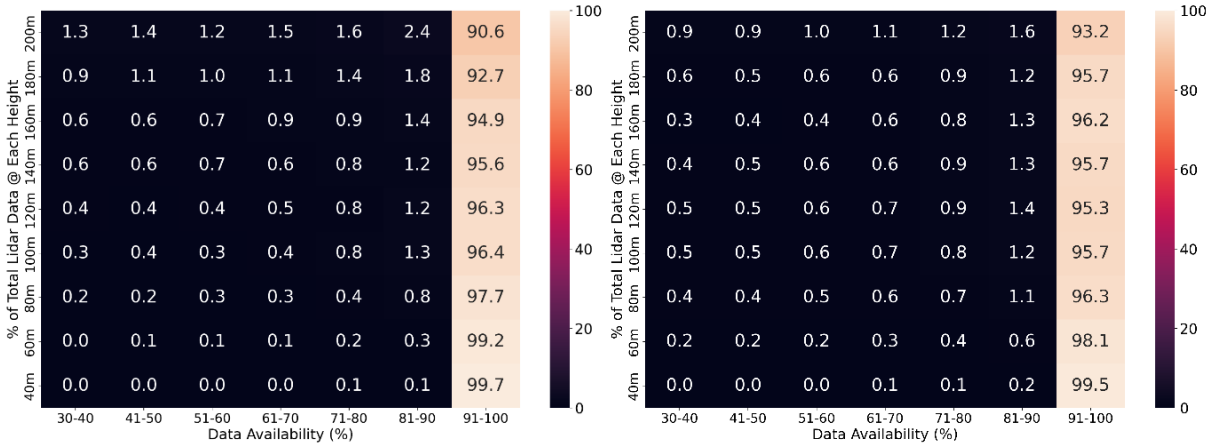

Figure 11. Frequency of bins of lidar data availability (x-axis) at each height (y-axis) for (left) Humboldt and (right) Morro Bay

Given these lidar data availability results at each height and location, we conclude that the impact of lidar data availability is neglectable.

2.6 Analysis of Cloud Coverage Conditions

In this section, we investigate whether cloud coverage conditions may be connected to some of the wind speed bias found in CA20. For this analysis, we use pyranometer data from the deployed lidars at both Humboldt and Morro Bay. A pyranometer measures irradiance from the sun; therefore, high values (>600 watts per square meter [W/m^2]) are indicative of sunny, cloud-free conditions, and lower values are indicative of cloudy conditions. Values of zero occur at night.

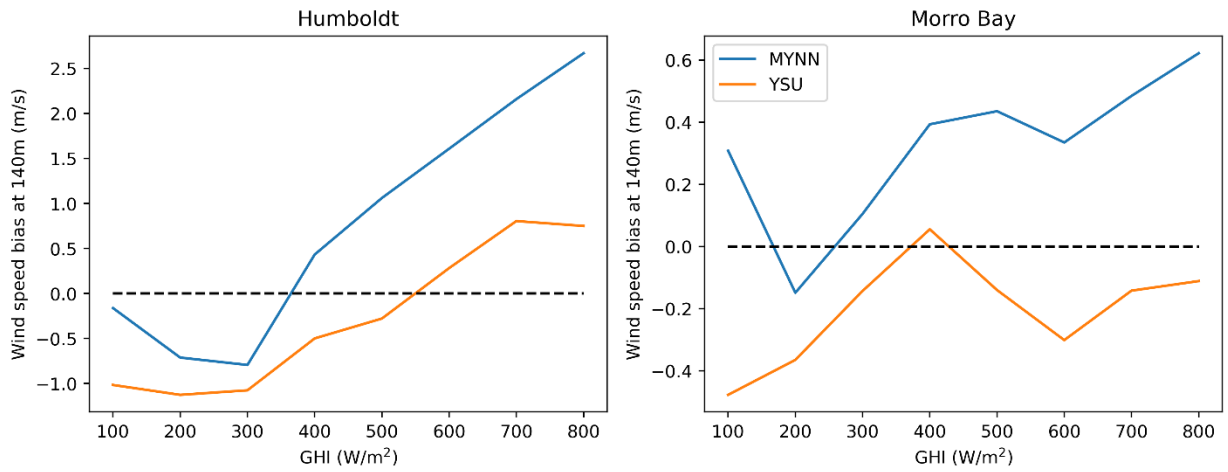

Figure 12. Modeled 140-m wind speed bias as it relates to observed global horizontal irradiance (GHI) at (left) Humboldt and (right) Morro Bay

We explore the impact of cloud cover on wind speed bias in Figure 12, where we plot mean biases as a function of binned values of global horizontal irradiance (GHI). Here, we only include data between the hours of 10:00 and16:00 local time to remove diurnal trends in GHI (i.e., peaks at midday, lows at sunrise/sunset). We see that, in general, the bias grows positively with higher irradiance, or lower cloud cover. This is more pronounced at Humboldt than at Morro Bay.

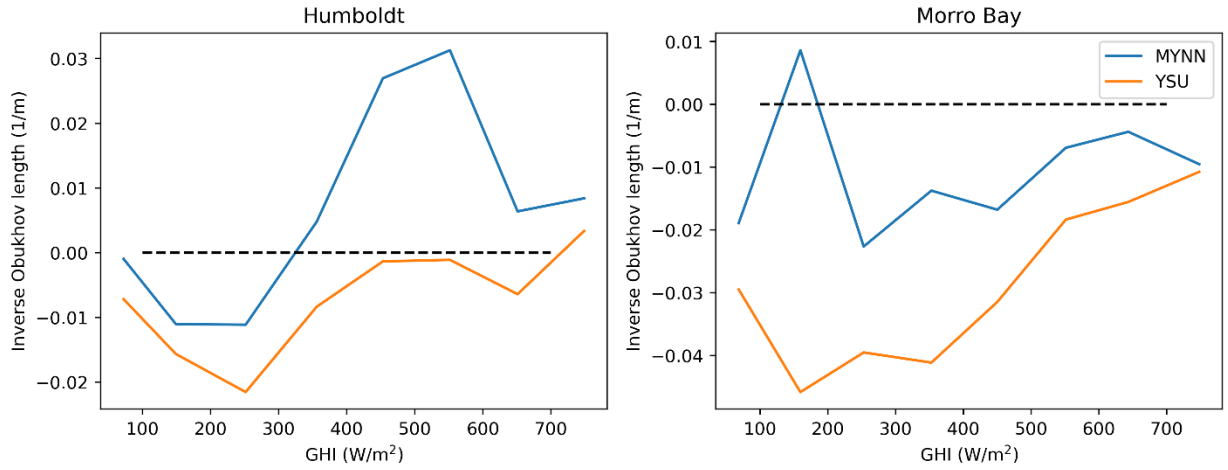

Figure 13. Relationship between observed GHI and modeled atmospheric stability (quantified as inverse Obukhov length) at (left) Humboldt and (right) Morro bay

The trend in bias with cloud cover is explained by the fact that cloud cover is strongly tied to offshore atmospheric stability, especially at Humboldt. In Figure 13, we see that the modeled inverse Obukhov length at 2 m (a measure of atmospheric stability) is positively correlated with GHI, i.e., we tend to see more stable conditions during offshore clear-sky conditions, especially at Humboldt. Because wind speed bias is so strongly tied to atmospheric stability, as detailed in the previous sections, we also see a strong trend with cloud cover conditions, especially at Humboldt.

2.7 Validation Against Available Onshore Observations

To further confirm the improved performance of the YSU-based runs over the MYNN-based runs, we extended the model validation to include available onshore observations, in addition to the offshore lidar-based validation. Specifically, we reviewed coastal radar measurements from the National Oceanic and Atmospheric Administration (NOAA). These radars provide hourly wind speed measurements starting at about 190 m above ground level at several locations across the California coastline. NREL reviewed the data for overlap between the extended CA20 time period (i.e., October 2020 through September 2021) and identified two radar data sources that would be suitable for validation: McKinleyville and Bodega Bay, the locations of which are shown in Figure 14.

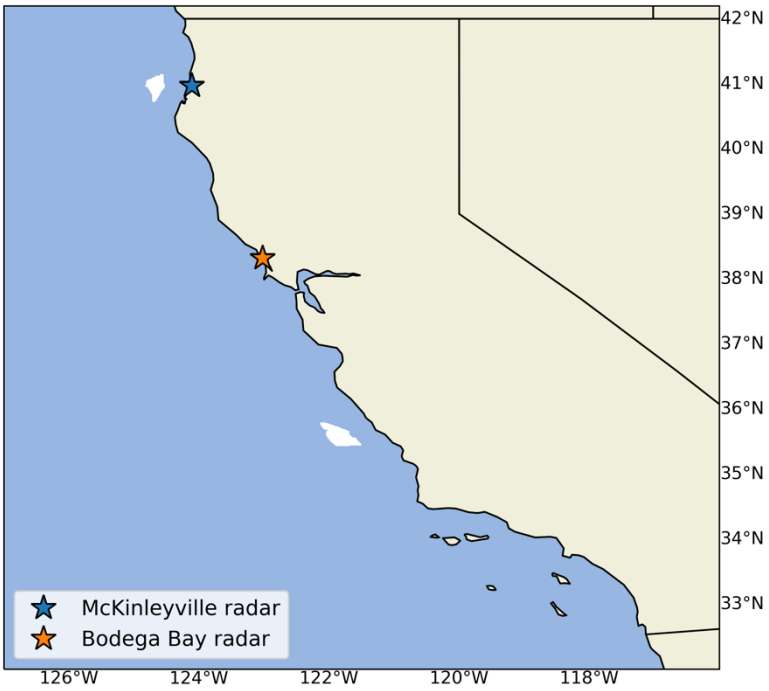

Figure 14. Locations of coastal radar stations used for extended validation of the WRF data sets

Results of this validation at 195 m, summarized in Table 1, show how the YSU-based simulation outperforms the MYNN-based runs at both radar locations and across all performance metrics. However, we notice that the performance metrics are generally poorer than those found for the offshore lidar validation. This likely relates to the proximity of the radar stations to the coastline and the fact that the WRF runs are at 2-km resolution. At this resolution, WRF is not able to accurately resolve the sharp gradient in wind speeds within the land-sea transition area and is likely leading to these relatively poor performance metrics, thus suggesting that the use of floating lidar should be considered, in general, as the optimal way to validate offshore wind resource assessment models.

Table 1. Results of the Validation of Extended CA20 Modeled 195-m Wind Speeds at Two Coastal Radar Locations

	MYNN-Based WRF	YSU-Based WRF
McKinleyville		
Bias	1.83 m/s	1.33 m/s
cRMSE	3.77 m/s	3.19 m/s
R^2	0.50	0.52
Bodega Bay		
Bias	0.96 m/s	0.78 m/s
cRMSE	3.07 m/s	2.94 m/s
R^2	0.71	0.72

2.8 Meteorological Drivers in Select Short-Term Case Studies

Finally, we further explored the identification of additional meteorological drivers that contribute to enhancing the modeled wind speed bias in specific short-term case studies. The results of this analysis are summarized in Liu et al. (2023).

3 An Updated Data Set for the California Pacific Outer Continental Shelf

Given the results of the analysis described above, NREL has produced an updated offshore wind resource assessment data set for the region, which has replaced CA20. The updated data set is part of NREL's 2023 National Offshore Wind (NOW-23) data set, which is a 20+ year data set for all U.S. offshore waters (except for Alaska). The production of the NOW-23 data set, including its regional domain for offshore California (also called South Pacific within the NOW-23 national context) is described in Bodini et al. (in review).

The NOW-23 data set for offshore California is available from January 1, 2000, to December 31, 2022. As detailed in the previous section, it adopts the ERA-5 reanalysis product, the YSU PBL scheme, the MM5 surface layer scheme, and the NOAH land surface model. As far as the sea surface temperature forcing, we adopt a high-resolution version of the OSTIA data set, where data are interpolated at hourly resolution from OSTIA's native daily resolution.

The 23-year mean wind speed at 160 m above sea level (a.s.l.) for the region is shown in Figure 15, taken from Bodini et al. (in review), which also describes the seasonal and diurnal variabilities of the offshore wind resource in the region.

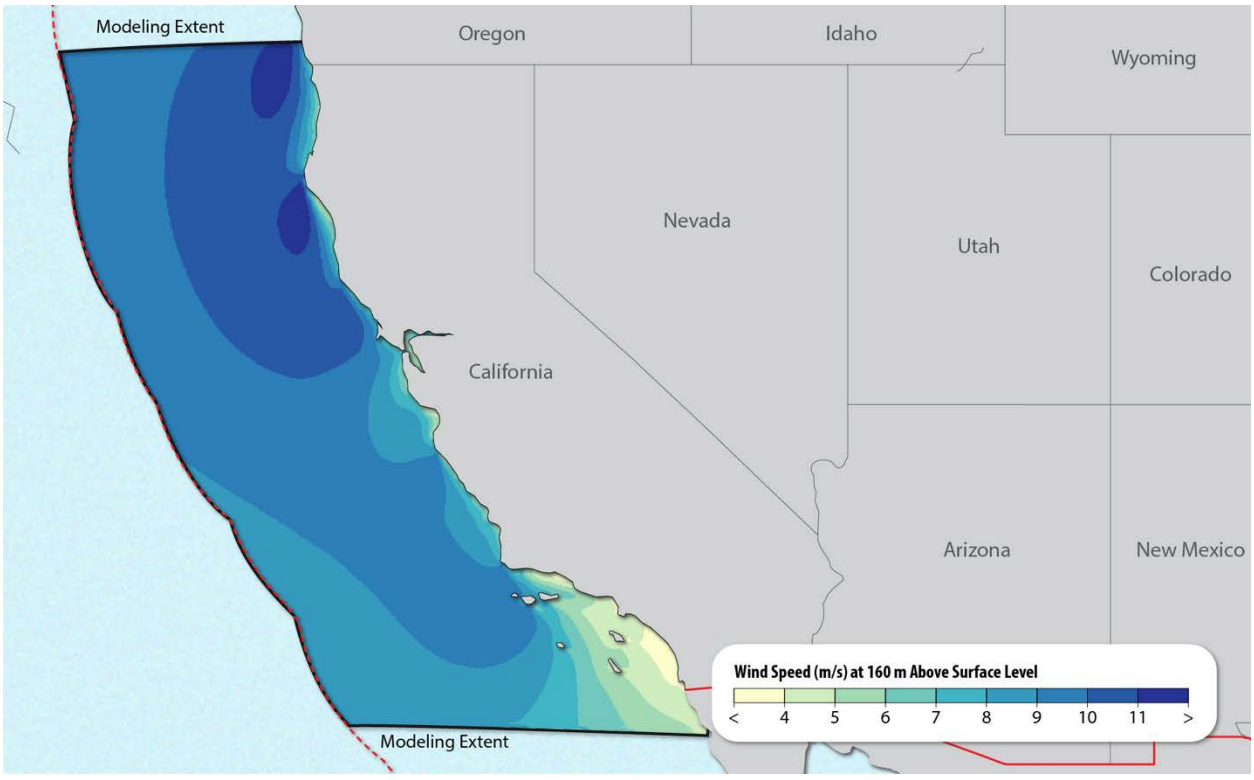

Figure 15. Map of the 23-year (2000–2022) mean wind speed at 160 m a.s.l. for the South Pacific region. The red dashed line represents the limit of the U.S. exclusive economic zone (EEZ). The continuous black line, where not overlaid with the EEZ boundary, shows the limit of the NOW-23 WRF domain. Taken from Bodini et al. (in review).

Additionally, we show in Figure 16 the difference in mean wind speed at 160 m a.s.l. between NOW-23 (2000–2022) and the now-deprecated CA20 data set (2000–2019). We observe that NOW-23 models, on average, lower wind speed across the whole region, with the largest difference (close to 1.5 m/s), in northern California, near the Humboldt wind energy lease area.

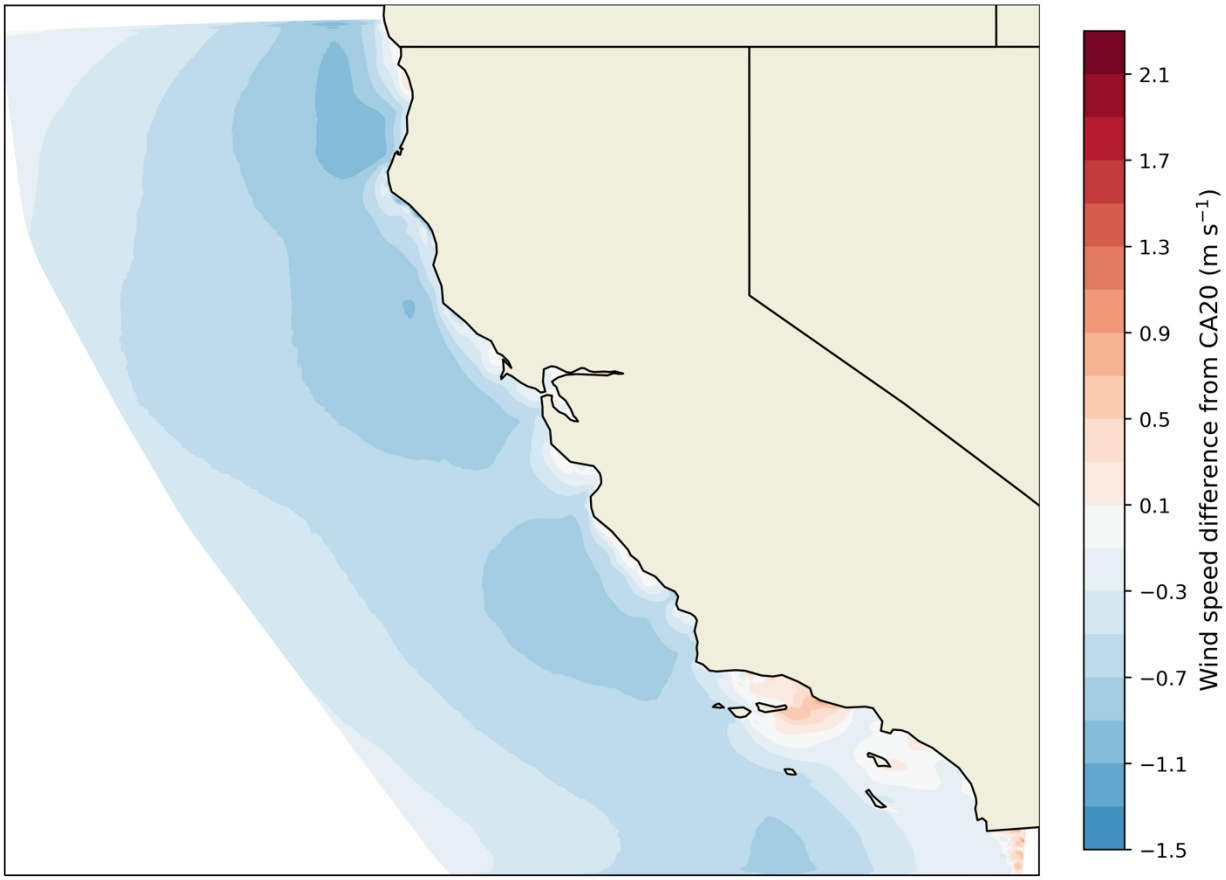

Figure 16. Map of the difference in mean wind speed at 160 m a.s.l. between the 23-year (2000–2022) NOW-23 data set and the 20-year (2000–2019) now-deprecated CA20 data set. Taken from Bodini et al. (in review).

As previously described, the new model setup validates well against available offshore observations. Figure 17 shows vertical profiles of bias, cRMSE, and R^2 between NOW-23 and concurrent lidar observations at Humboldt and Morro Bay. The new modeled data have a negligible bias at both locations and at all heights, which represents a significant improvement compared to the now-deprecated CA20 data set.

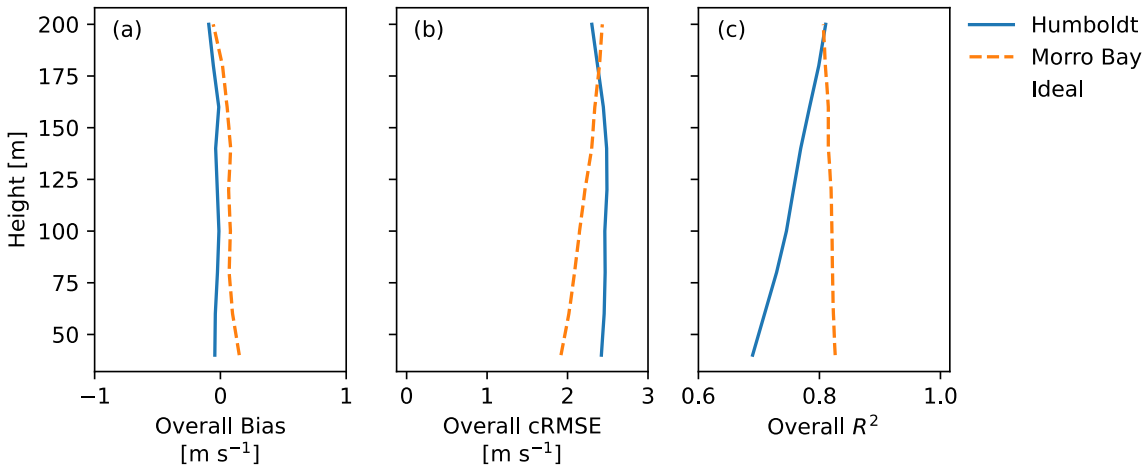

Figure 17. (a) Bias, (b) cRMSE, and (c) R^2 calculated at Humboldt and Morro Bay for NOW-23 compared to the concurrent floating lidar observations

4 Conclusions and Next Steps

The analysis completed has shown that atmospheric stability is a key factor in explaining the long-term bias in the CA20-modeled wind resource relative to floating lidar observations in offshore California. Specifically, we found that offshore California is dominated by extremely stable conditions, with low turbulence and limited vertical mixing, which lead to high wind speed at hub height and frequent low-level jets. During these stable conditions, different PBL schemes diverge, so that it is reasonable to expect a lower bias when using the PBL scheme that more accurately represents atmospheric stability. We found that the MYNN scheme models higher stability than YSU, and near the surface it overestimates stability compared to observations, thus resulting in too-strong mean wind speeds at hub height.

Additionally, for select short-term case studies, we found that other meteorological drivers contribute to the observed bias in hub-height wind speed. In these case studies, when the wind conditions at Humboldt are characterized by synoptic-scale northerly flows driven by the North Pacific High and inland thermal low, we observe a coastal warm bias in the MYNN simulations. This enhanced land-sea temperature gradient contributes to the modeled wind speed bias by altering the boundary layer thermodynamics via a thermal wind mechanism.

Given the strong performance of the YSU-based runs, NREL published an updated version of the offshore California data set using the YSU setup. This new data set has replaced the original CA20 and is part of the NOW-23 data set that NREL recently published.

A recommended next step, which would require additional research funding, is assessing the potential bias in the NOW-23 data set in Hawaii and the Pacific Northwest. Both these data sets were run with the same MYNN parameterization as CA20 and were not validated against observations. In Hawaii, a recent lidar deployment would allow for a validation of the MYNN model setup to assess whether a rerun of the full 20-year data set is recommended. In the Pacific Northwest region, the lack of lidar observations remains a critical issue. A more careful validation using available buoy and coastal observations could still be leveraged to better assess the skills of the existing modeled data set in the region.

More broadly, additional analysis is needed to fully understand why MYNN is failing in very stable conditions and whether this poor performance could more broadly affect all the regions where the PBL scheme is chosen. This aspect is particularly concerning because the atmospheric science community has largely embraced MYNN as the go-to PBL scheme for many wind-energy-related applications: MYNN is in fact adopted in NOAA's High-Resolution Rapid Refresh model and the New European Wind Atlas, among other applications.

References

Bodini, N., M. Optis, S. Redfern, D. Rosencrans, A. Rybchuk, J. K. Lundquist, V. Pronk, et al. In review. "The 2023 National Offshore Wind Data Set (NOW-23)." *Earth System Science Data Discussions*. https://essd.copernicus.org/preprints/essd-2023-490/.

Bodini, N., A. Rybchuk, M. Optis, W. Musial, J. K. Lundquist, S. Redfern, C. Draxl, R. Krishnamurthy, and B. Gaudet. 2022. *Update on NREL's 2020 Offshore Wind Resource Assessment for the California Pacific Outer Continental Shelf*. Golden, CO: National Renewable Energy Laboratory. NREL/TP-5000-83756. https://doi.org/10.2172/1899984.

Krishnamurthy, R., G. García Medina, B. Gaudet, W. I. Gustafson Jr., E. I. Kassianov, J. Liu, R. K. Newsom, L. M. Sheridan, and A. M. Mahon. 2023. "Year-long Buoy-Based Observations of the Air–Sea Transition Zone off the U.S. West Coast" (Preprint). *Earth System Science Data Discussions*. https://essd.copernicus.org/articles/15/5667/2023/essd-15-5667-2023.html.

Liu, Y., B. Gaudet, R. Krishnamurthy, S.-L. Tai, L. K. Berg, N. Bodini, A. Rybchuk, and A. Kumler. 2023. "Identifying Meteorological Drivers for Errors in Modeled Winds Along the Northern California Coast." *Monthly Weather Review* (in press). https://doi.org/10.1175/MWR-D-23-0030.1.

Muñoz-Esparza, D., B. Cañadillas, T. Neumann, and J. Van Beeck. 2012. "Turbulent Fluxes, Stability and Shear in the Offshore Environment: Mesoscale Modelling and Field Observations at FINO1." *Journal of Renewable and Sustainable Energy* 4(6): 063136. https://doi.org/10.1063/1.476920.

Optis, M., A. Rybchuk, N. Bodini, M. Rossol, and W. Musial. 2020. *2020 Offshore Wind Resource Assessment for the California Pacific Outer Continental Shelf*. Golden, CO: National Renewable Energy Laboratory. NREL/TP-5000-77642. https://doi.org/10.2172/1899984.

Sheridan, L. M., R. Krishnamurthy, G. García Medina, B. J. Gaudet, W. I. Gustafson Jr., A. M. Mahon, W. J. Shaw, R. K. Newsom, M. Pekour, and Z. Yang. 2022. "Offshore Reanalysis Wind Speed Assessment Across the Wind Turbine Rotor Layer off the United States Pacific Coast." *Wind Energy Science* 7: 2059–2084. https://doi.org/10.5194/wes-7-2059-2022.

Sheridan, L. M., R. Krishnamurthy, A. M. Gorton, W. J. Shaw, and R. K. Newsom. 2020. "Validation of Reanalysis-Based Offshore Wind Resource Characterization Using Lidar Buoy Observations." *Marine Technology Society Journal* 54(6): 44–61. https://doi.org/10.4031/MTSJ.54.6.13.